A Macroscopic Model for Countercurrent Gas-Liquid Flow in Packed Columns

A macroscopic model based on the volume-averaged equations of motion is presented for countercurrent gas-liquid flow in a packed bed. The model yields a column-limited flooding point as the loss of existence of uniform states. It correctly predicts the existence of two uniform states below the flooding point. The lower branch corresponds to the trends commonly observed experimentally. It is shown that the upper branch is made unattainable by the gas distributor/support plate at the bottom of the column. The occurrence of premature flooding induced by the support plate is also explained. It is suggested that the occurrence of spontaneous liquid segregation, necessitating frequent liquid redistribution in columns with large dumped packings and porosities, is a consequence of the loss of stability of the uniform state in the lower branch.

David C. Dankworth
S. Sundaresan
Department of Chemical Engineering
Princeton University
Princeton, NJ 08544

Introduction

The study of two-phase flow of gas and liquid in packed columns has received attention due to its importance in many industrial processes. The countercurrent regime, where liquid flows downward while gas flows upward through the packing, has been studied extensively since the early 1930's. Modeling of two-phase flow in packed beds is carried out mostly by correlating experimental observations and applying the correlation to predict pressure drop, holdup, or flooding point. This remains valuable as a practical method for design of packed towers. The correlation approach, however, often reveals little about possible mechanisms behind the various hydrodynamic phenomena observed. Usually, different correlations must be used to predict each property or phenomenon. From a theoretical standpoint, a single model capable of accounting for all the observed behavior would have advantages over the more or less empirical correlations.

The flooding point is one characteristic of countercurrent flow that is of prime importance in determining the maximum capacity of a packed column. Flooding in packed columns can be defined as the conditions where no further increase in gas or liquid flow rate through the packing can be made without decreasing the flow of the other phase. An increase in the external flow to a flooded column will result in accumulation of liquid at the top of the bed. The flooding point was originally correlated by Sherwood et al. (1938), and some form of this correlation, slightly modified by Lobo et al. (1945) to better account for particle geometry, is still in use today. These correlations must be used cautiously, however, as flooding can be prematurely brought on by improper design of the support plate at the bottom of the tower. Qualitative arguments to explain support-plate-induced flooding have been given by Eckert (1970). No theoretical attempts to model the effect of the support plate have been presented previously.

Commercial packed towers usually employ large, high-voidage packing materials such as saddles or rings. It is known that the flow is not uniform in some of these commercial packings, making it necessary to redistribute the liquid at intervals along the tower (Eckert, 1961). The reason why such spontaneous segregation occurs in these columns is not well understood.

Previous attempts to model countercurrent flow have focused on trying to give a theoretical basis to the correlations. Davidson (1959) and Buchanan (1967) developed a model for liquid holdup based on the flow of liquid films down inclined surfaces. Hutton and Leung (1974a) combined this type of holdup model with a correlation for gas-phase pressure drop to obtain a model for the uniform steady-state holdup and pressure drop. In their model, flooding was interpreted as the point where the derivative of liquid flow rate with respect to liquid holdup is zero. They have also applied their model to cocurrent flow with some success (Hutton and Leung, 1974b). Implicit in that definition of flooding is the existence of two steady operating states for given gas and liquid mass flow rates. One of these corresponds to the

Correspondence concerning this paper should be addressed to S. Sundaresan.

state usually found in operation of packed beds, while the other exists at higher liquid holdup and higher pressure drop. Hutton and Leung (1974c) have found some experimental evidence for the existence of the latter state and have concluded that it is unstable.

A macroscopic model for two-phase flow through packed columns can be readily formulated by volume-averaging of the equations of motion for each phase. Since such a model is formulated without any special assumption about the direction of flow, it can be applied for cocurrent downflow or upflow as well as for countercurrent flow. The model has already been applied with some success to cocurrent downflow by Grosser et al (1988). This work demonstrated the ability of the model to predict the transition between the trickling and pulsing flow regimes in trickle beds. In the present study, we will show that the same macroscopic model can be used to elucidate several qualitative features characterizing countercurrent flow:

- The occurrence of flooding
- The profound effect of the bottom gas distributor/support plate on the flooding conditions
- The occurrence of spontaneous maldistributions in some columns with large porosities and packing sizes

In this paper, we will first describe the mathematical model which consists of the volume-averaged continuity equations and momentum balances for each phase, outline the method for analyzing the hydrodynamic stability of uniform flow, and present the algebraic criterion for stability to small disturbances. Analysis of the model will reveal that there are two possible values of uniform liquid holdup and pressure drop which satisfy the equations for each countercurrent flow condition. It will be shown that the hydrodynamic stability of the uniform flow can be significantly influenced by the particle size and shape. The state of uniform flow becomes unstable as the porosity and particle size are increased. The model predicts the absence of a stable uniform state for the porosity and packing sizes commonly used in industrial-packed columns.

The conditions for column-limited flooding will naturally arise from the model as the conditions where no uniform solution exists. The model predicts flooding at flow rates higher than observed experimentally, indicating that other factors bring about premature flooding. We then address the problem of a restrictive support plate at the bottom of the bed and show that excess holdup at the bottom support plate can produce time-dependent flow and flooding at conditions less severe than the limiting flow rates.

Finally, we discuss the nature of the upper uniform state. Although this state is generally unstable and not observed, it is possible to artificially induce a column to operate at high liquid holdup and pressure drop. The time-dependent flow obtained has average properties very similar to those of the upper uniform flow conditions. This is compared with experimental data.

Macroscopic Model

A macroscopic model for gas-liquid flow in packed columns has been proposed by Grosser et al. (1988). The full model consists of the volume-averaged equations of motion for each phase, along with appropriate constitutive relations. It is expected that such a model should be valid when both phases are continuous and packing size is small compared to overall bed dimensions, as is found in packed columns under most conditions.

For a uniformly packed column of porosity ϵ, if both phases are assumed to be incompressible, the continuity and momentum balances in terms of volume fraction occupied by each phase ϵ_i and local mean velocities u_i are:

$$\epsilon_l + \epsilon_g = \epsilon \tag{1}$$

$$\frac{\partial \epsilon_i}{\partial t} + \nabla \cdot (\epsilon_i \underline{u}_i) = 0, \quad i = l, g \tag{2}$$

$$\rho_i \epsilon_i \left[\frac{\partial \underline{u}_i}{\partial t} + \underline{u}_i \cdot \nabla \underline{u}_i\right] = -\epsilon_i \nabla p_i + \epsilon_i \rho_i \underline{g} + \underline{F}_i + \epsilon_i \nabla \cdot \underline{\tau}_i + \nabla \cdot \underline{R}_i, \quad i = l, g \tag{3}$$

The last two terms on the righthand side of the momentum balance equation represent contributions due to mean viscous and pseudoturbulence stresses. It can be shown through simple scaling arguments that these terms are small compared to the interfacial drag force and pressure gradient terms. Therefore, as a first approximation we will ignore them in our analysis.

Semiempirical constitutive models for the interphase drag force terms, $\underline{F}_i$, have been developed by Saez and Carbonell (1985):

$$\underline{F}_g = -\left\{\frac{A\mu_g(1-\epsilon)^2\epsilon^{1.8}}{d_e^2\epsilon_g^{2.8}} + \frac{B\rho_g(1-\epsilon)\epsilon^{1.8}}{d_e\epsilon_g^{1.8}}|\underline{u}_g|\right\}\underline{u}_g \tag{4}$$

$$\underline{F}_l = -\left\{\frac{\epsilon - \epsilon_l'}{\epsilon_l - \epsilon_l'}\right\}^{2.43}\left\{\frac{A\mu_l(1-\epsilon)^2\epsilon_l^2}{d_e^2\epsilon^3} + \frac{B\rho_l(1-\epsilon)\epsilon_l^3}{d_e\epsilon^3}|\underline{u}_l|\right\}\underline{u}_l \tag{5}$$

where d_e is the effective particle diameter, and A and B are Ergun coefficients. The static holdup is the volume fraction of liquid in the bed with no flow and can be estimated as

$$\epsilon_l' = \frac{1}{(20 + 0.9\,Eo^*)} \tag{6}$$

where the Eötvos number is given by

$$Eo^* = \frac{\rho_l g d_e^2 \epsilon^2}{\sigma(1-\epsilon)^2}. \tag{7}$$

It should be noted that the model is not specific to these correlations, but can be implemented with any suitable constitutive relation for the drag force terms. For example, a drag force correlation can also be derived for the Hutton and Leung (1974a) model, as shown in Eqs. 8 and 9.

$$F_g = -\left[\frac{8.5\mu_g a_v^2 u_g}{\rho_g} + \frac{a_v u_g^2}{\rho_g \epsilon_g}\left(\frac{\mu_g a_v \epsilon_g}{u_g}\right)^{0.1}\right]\frac{1}{\epsilon_g^3} \tag{8}$$

$$F_l = -S'\frac{u_l}{\epsilon_l}\left\{\frac{\rho_l}{d_e}\left[\rho_l g - \frac{F_g}{\epsilon_g}\right]\right\}^{1/2} \tag{9}$$

S' is a packing factor which depends on packing geometry. The above drag force relations are written for positive axial velocity defined in the direction of gravity. For countercurrent flow, the gas velocity will be negative in these relations, as well as in the model equations.

An additional relation exists between the pressure in each

phase. It was suggested by Grosser et al. (1988) that the capillary pressure may be approximated by Leverett's J function (Leverett, 1941):

$$p_c = p_g - p_l = \left[\frac{\epsilon}{k}\right]^{1/2} \sigma J(\epsilon_l) \tag{10}$$

The intrinsic permeablity, k, can be related to the Ergun parameter, A, by the relation

$$\left(\frac{\epsilon}{k}\right)^{1/2} = \frac{(1-\epsilon)}{\epsilon d_e}\sqrt{A}. \tag{11}$$

Leverett's J function data can be described reasonably well by (Grosser et al., 1988)

$$J(S_l) = 0.48 + 0.036 \ln\left[\frac{1-S_l}{S_l}\right]. \tag{12}$$

Here the drainage curve has been chosen as the appropriate curve for use in this model. This choice is discussed in Grosser et al. (1988). Leverett based his correlation upon experiments in porous media, using very small particles with correspondingly small pore size. Support for the use of this form for capillary pressure in beds of larger particles is provided by Reed et al. (1987), who have measured the capillary pressure in beds of up to 1-mm-diameter particles and have found that Leverett's correlation also describes these systems.

In this paper we shall restrict our attention to a one-dimensional flow problem and assume the flow is uniform in the lateral directions. Taking only the axial component of Eqs. 2 and 3 results in the following one-dimensional equations for each phase, where the z axis is directed vertically downward.

$$\frac{\partial \epsilon_i}{\partial t} + \frac{\partial \epsilon_i u_{iz}}{\partial z} = 0 \tag{13}$$

$$\rho_i \epsilon_i \left[\frac{\partial u_{iz}}{\partial t} + u_{iz}\frac{\partial u_{iz}}{\partial z}\right] = -\epsilon_i \frac{\partial p_i}{\partial z} + F_{iz} + \rho_i \epsilon_i g \tag{14}$$

For a bed of finite length, suitable boundary conditions must be specified at the top and bottom of the bed to make this one-dimensional model well posed. In a very long column, however, the conditions at the boundaries may not have a large effect on the conditions in the middle of the column. In this case, the interior of the packed bed can be approximated by a domain of infinite length, with the only conditions being that all velocities, volume fractions, and pressure gradients be bounded over the entire domain. A completely uniform solution is possible for such an infinite column. The uniform state is given by the conditions where all time derivatives are zero, and all holdup and velocity gradients vanish:

$$\frac{\partial p_i^o}{\partial z} = \frac{F_{iz}^o}{\epsilon_i^o} + \rho_i g. \tag{15}$$

If the equation for the liquid phase is subtracted from that for the gas phase, the lefthand side becomes the gradient in capillary pressure. Under uniform conditions, the capillary pressure is constant, leading to the following algebraic equation which can be used to calculate the properties of the uniform state.

$$0 = \frac{F_{gz}^o}{\epsilon_g^o} - \frac{F_{lz}^o}{\epsilon_l^o} + (\rho_g - \rho_l)g \tag{16}$$

where the superficial mass fluxes L, G are given by

$$G = -\rho_g \epsilon_g^o u_{gz}^o; \quad L = \rho_l \epsilon_l^o u_{lz}^o \tag{17}$$

The sign of G is chosen so that $G > 0$ for countercurrent flow. The uniform state may not be the only solution to Eqs. 13 and 14. In particular, there may also be time-dependent solutions.

To determine whether or not uniform flow will exist for given parameters, we can examine the hydrodynamic stability of the uniform state. The full derivation of the linear stability analysis is given in Grosser et al. (1988). The essential results are summarized here. In the analysis, the velocity, volume fraction, and pressure are expressed in terms of perturbations from the uniform state. Equations 1, 13, and 14 are then combined and linearized, and a spatially periodic normal mode solution is imposed of the form

$$y^* = \hat{y} \exp(st + j\omega z), \quad y = u_i, \epsilon_i, p_i \tag{18}$$

where ω is the wave number of the perturbation, and $s = s(\omega)$ is the complex wave velocity, which is to be determined. The real part of s describes the growth of a disturbance in time. If the real part of s is greater than zero, the system is unstable. The imaginary part of s can be identified with a wave propagation velocity. Substitution of Eq. 18 into the linearized form of Eqs. 13–14 gives, upon simplification, a polynomial in s and ω.

$$W_1 s^2 + s(W_2 + 2j\omega W_3) - \omega^2 W_4 - j\omega W_5 = 0 \tag{19}$$

where W_i terms are constants which depend on the properties of the uniform state, the fluid and bed properties, and the external mass fluxes L and G.

$$W_1 = \frac{\rho_g}{\epsilon_g^o} + \frac{\rho_l}{\epsilon_l^o} \tag{20}$$

$$W_2 = -\left[\frac{\alpha_g}{(\epsilon_g^o)^2} + \frac{\alpha_l}{(\epsilon_l^o)^2}\right] \tag{21}$$

$$W_3 = \frac{\rho_g u_{gz}^o}{\epsilon_g^o} + \frac{\rho_l u_{lz}^o}{\epsilon_l^o} \tag{22}$$

$$W_4 = \frac{\rho_g (u_{gz}^o)^2}{\epsilon_g^o} + \frac{\rho_l (u_{lz}^o)^2}{\epsilon_l^o} + \left[\frac{\epsilon}{k}\right]^{1/2} \sigma J'(\epsilon_l^o) \tag{23}$$

$$W_5 = \frac{F_{gz}^o}{(\epsilon_g^o)^2} + \frac{F_{lz}^o}{(\epsilon_l^o)^2} - \frac{\beta_l}{\epsilon_l^o} - \frac{\beta_g}{\epsilon_g^o} + \frac{\alpha_g u_{gz}^o}{(\epsilon_g^o)^2} + \frac{\alpha_l u_{lz}^o}{(\epsilon_l^o)^2} \tag{24}$$

where

$$\alpha_i = \left[\frac{dF_{iz}}{du_{iz}}\right]^o; \quad \beta_i = \left[\frac{dF_{iz}}{d\epsilon_i}\right]^o, \quad i = l, g \tag{25}$$

$$J'(\epsilon_l^o) = \left[\frac{dJ}{d\epsilon_l}\right]^o \tag{26}$$

Solution of Eq. 19 results in an algebraic criterion for stability in terms of the constants W:

$$W_1W_5^2 + 2W_2W_3W_5 + W_2^2W_4 \leq 0 \qquad (27)$$

When Eq. 27 is satisfied, the uniform state solution is stable to small periodic perturbations.

Uniform-State Locus

The uniform state described by Eq. 16 is the condition where all the dominant forces in the bed are balanced. The uniform state relation can be used to determine the properties of the flow, such as liquid holdup, pressure gradient, and stability, given the external conditions of gas and liquid mass fluxes. Experimental data are usually taken with one of these fluxes fixed, while the other is varied over a range. A similar presentation can be constructed from Eq. 16, using an appropriate relation for the drag forces, such as Eqs. 4–5, or the Hutton and Leung model given by Eqs. 8 and 9. By holding liquid flux constant, a locus of uniform-state conditions can be obtained for a range of gas fluxes. Figure 1 shows such a plot for a bed of 12.5-mm spheres at a constant liquid flux of 15 kg/m^2 · s. The parameter values used in the simulations are shown in Table 1. Uniform state curves for both Hutton and Leung (1974a), and Saez and Carbonell (1985) drag force correlations are shown. Both relations reveal the same qualitative features. The existence of two uniform states for each gas mass flux, and a limiting gas mass flux, beyond which no uniform state solutions are possible, are readily apparent from Figure 1, and this has already been pointed out by Hutton and Leung (1974a, c).

Figure 2 shows the pressure gradient predicted by the model for 6-mm spheres using the Saez and Carbonell drag force correlations (Eqs. 4 and 5). Note that the pressure gradient can also have two values for each flow condition. Although the uniform-state model predicts the existence of two uniform states, only one state is observed in real columns. Pressure drop and liquid holdup generally increase with increasing flow rate of either phase. The corresponding family of curves for liquid holdup is shown in Figure 3. The experimentally observed behavior qualitatively follows the lower branch, while the upper branch is not observed as steady uniform flow.

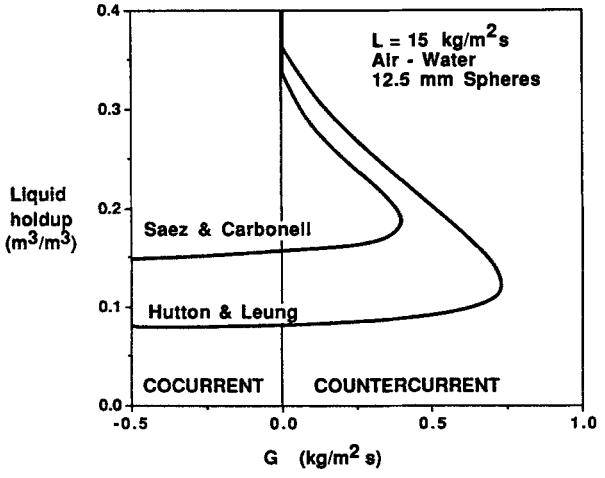

Figure 1. Uniform state curves for liquid holdup as a function of gas mass flux at constant liquid mass flux.

Comparison of two drag force correlations. Model parameter values are given in Table 1.

Table 1. Parameter Values Used in the Simulations

$A = 180$	$\rho_g = 1.17$ kg/m^3
$B = 1.8$	$\rho l = 1000$ kg/m^3
g = 9.8 m/s^2	$\mu_g = 1.84 \times 10^{-5}$ kg/m · s
$\sigma = 7.15 \times 10^{-2}$ kg/s^2	$\mu_l = 10^{-3}$ kg/m · s
Spheres	
$\epsilon = 0.4$	$d_e = 0.006$ m (Unless stated)
$S' = 1.8$	

It can be seen in Figures 2 and 3 that, as the liquid flux is increased, the curves move to lower gas flux and higher liquid holdup, as one would expect. The figures also show that the flooding point must occur at lower gas flux as the liquid rate is increased. For high-enough liquid flux, the curve lies flat against the vertical axis. This is reasonable, since there is a limit to the liquid flux that can be passed through the column under the influence of gravity alone.

At low gas flux, the holdup is strongly dependent on liquid velocity, but is almost independent of gas velocity. Uniform-state curves can also be calculated for constant gas rate conditions. Figure 4 shows such curves for 12.5-, 18.75- and 25.4-mm spheres. Also shown are data from Jesser and Elgin (1943) for the same particle sizes. The model predictions are consistently higher than the measured values, but the model curves follow the shape of the experimental curves very closely.

Stability and Packing Geometry

The stability of a specified uniform state can be determined using Eq. 27. This is illustrated in Figure 5, where the operating conditions predicted by the linear stability analysis to be stable are shown by solid lines and the unstable conditions are shown by broken lines. For fixed liquid flux in an infinite, one-dimensional bed, there can be a range of operating conditions which allow stable uniform solutions. The lower limit of this range

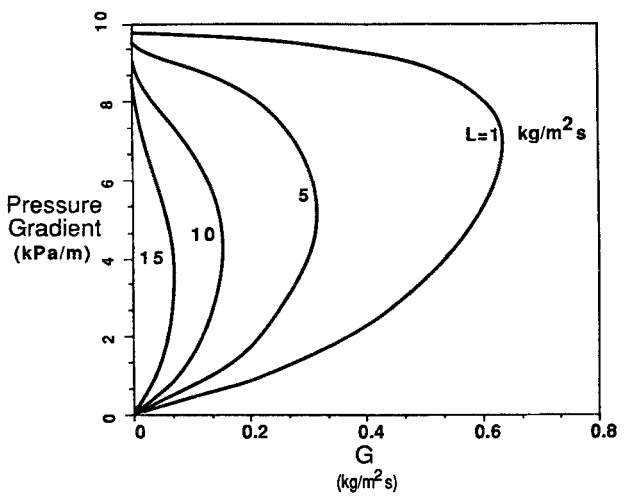

Figure 2. Variation of pressure gradient with gas mass flux at several constant liquid rates.

$d_e = 6$ mm.

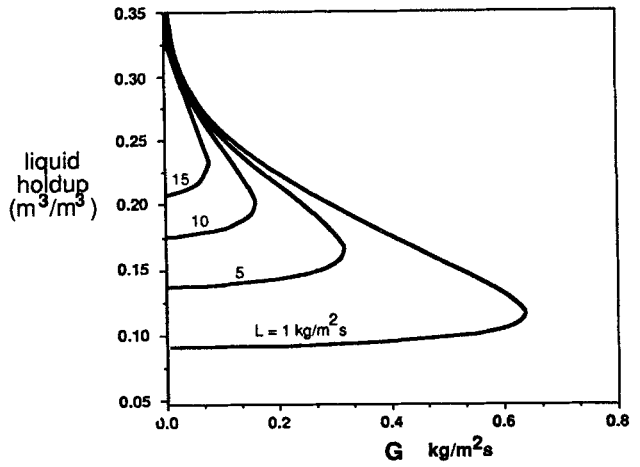

Figure 3. Variation of liquid holdup with gas flux for several constant liquid rates.
The values of other parameters are as in Table 1.

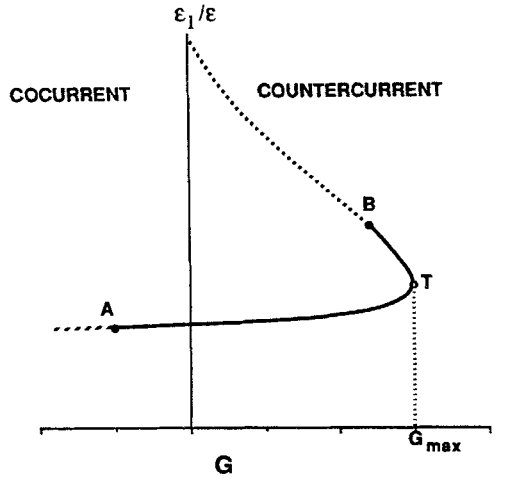

Figure 5. Uniform state locus.
Point A denotes trickling-to-pulsing transition in cocurrent downflow. G_{max} denotes the gas flux at the turning point corresponding to column-limited flooding conditions.

(point A) lies in the cocurrent downflow regime for small, spherical packing. The instability, which occurs as the cocurrent gas flux is increased past this limit, was associated with the trickling-to-pulsing transition by Grosser et al. (1988). The upper limit of the range always lies in the countercurrent regime on the upper half of the curve (point B), near the turning point of the uniform-state locus (point T). Thus, for small spheres, the lower half of the countercurrent uniform-state curve is completely stable, and the range of gas flux for which stable uniform flow is permissible is bounded by points A and T. As will be discussed later, the stability predicted by the analysis of an infinite column in the upper branch region between B and T is spurious, and this range of uniform state is not attainable in practice as inherently-stable operating points.

Other particle geometries can be examined by changing the model parameters for total bed porosity ϵ and effective particle size d_e. Commercial packed towers usually employ large, high-voidage packing materials, such as saddles or rings. It is known that the flow is not uniform in some of these commercial packings, making it necessary to redistribute the liquid at intervals along the tower (Eckert, 1961). When the model is applied to larger particles and higher total voidage, the predicted stability transitions change location. For fixed particle size, as the bed voidage is increased, the upper stability transition (point B) moves closer to the turning point of the curve (point T). Also, the lower transition (point A) moves from the cocurrent into the countercurrent regime, and rapidly approaches the upper transition. Eventually, for high porosity, the entire curve becomes unstable. This behavior is illustrated in Figure 6.

The region inside the curves in Figure 6 shows the range of gas flux for stable, uniform operation at a constant liquid flux of 5 kg/m² · s. For each particle size, the upper and lower boundaries shown in Figure 6 are simply the loci of G_{max} (point T) and point A in Figure 5, respectively. The maximum gas flux (G_{max}) increases with total voidage as there is more area for flow, but

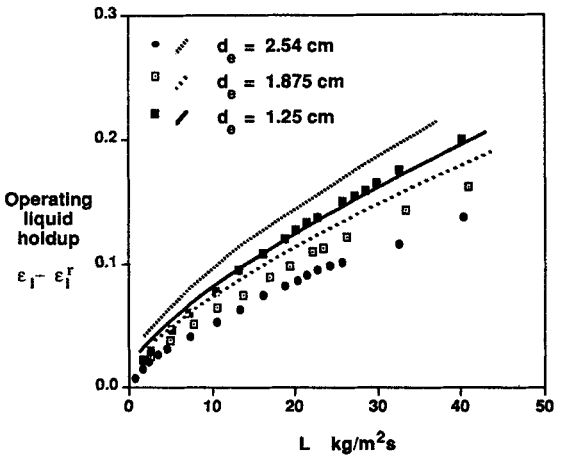

Figure 4. Comparison of experimental and predicted variation of liquid operating holdup with liquid flux for different packing diameters.
The data are from Jesser and Elgin (1943).
The drag force was obtained from Eqs. 4 and 5.

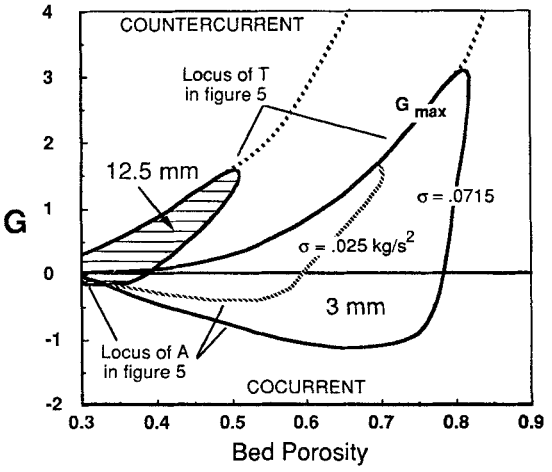

Figure 6. Dependence of the stability of the uniform state on total bed voidage.
The stable range of gas flux is shown as a function of bed voidage for constant liquid flux of 5 kg/m² · s, and two different effective particle diameters. Minimum stable gas flux curves are shown for interfacial tensions of 0.0715 and 0.025 kg/s² for the 3-mm particles.

eventually the minimum stable gas flux (point A) moves into the countercurrent region of the plot ($G > 0$). As bed porosity is increased further, the range of gas flux for a stable uniform flow shrinks rapidly until the uniform state locus becomes completely unstable. The voidage, at which complete loss of stability occurs, is lower for larger particles. Stable uniform flow is possible for up to 80% voids in a bed with 3-mm effective particle diameter, but is only possible up to 50% voids in a bed of 12.5-mm particles. Larger particles would lose stability at even lower void fraction for this liquid flux.

Figure 6 also shows the region of stable uniform operation for 3-mm particles at two different values of interfacial tension. The minimum stable gas flux curve moves closer to the maximum gas flux curve as the interfacial tension is decreased, and the complete loss of stability occurs at lower void fraction. The maximum gas flux curve is not greatly affected by changes in interfacial tension, which is consistent with experimental measurements of the effect of interfacial tension on the flooding point (Sherwood et al., 1938).

The loss of stability can be explained in terms of the balance between inertial and capillary forces. Inertial forces tend to destabilize the flow, while capillary forces tend to make the flow more uniform. The capillary pressure is very dependent on the size of the flow channels. It becomes very small when the flow channels get large, as in high-porosity, large-particle-size beds. These parameters have the opposite effect on the inertial forces. Therefore, as the flow channels get large, it becomes impossible for the capillary forces to counteract the inertial forces and instability results.

Commercial packings are usually larger than 12.5 mm in effective diameter and have voidage ranging from 55–96% (Eckert, 1970). If the model is correct, then we should not expect to find uniform flow in these columns. Even if uniform conditions were induced initially in such a column, any small disturbance from uniformity would tend to grow, forcing the flow away from a uniform state. The precise nature of the eventual flow conditions cannot be determined from a linear stability analysis, since the linearization of the equations is valid only for very small deviations from uniform conditions. It was found in our analysis that the amplification factor, s, in Eq. 18 is always complex except at the turning point, where it is real. This suggests that, when loss of stability occurs, the resulting flow will be time-dependent as well as axially-nonuniform. In an actual column, no time variation of pressure drop is observed for conditions below the flooding point. This is not reason to disbelieve the model, however, since in cocurrent pulsing, the pulses are observed to get very weak as the packing size is increased. Therefore, the transient nature of the flow may have an amplitude smaller than the precision of the measurement devices and, consequently, may have escaped detection in countercurrent flow experiments with large packings and porosities.

In formulating the one-dimensional model, we have assumed that the flow is uniform in the lateral directions. This assumption may also become invalid when the uniform axial solutions are unstable. The resulting flow could easily be two- or three-dimensional, depending on whether stable, laterally-nonuniform flow is possible. The loss of stability of the uniform state shown by the model could be interpreted as a tendency toward segregation of the phases, possibly explaining the mechanism of the observed maldistribution of liquid in these packings. It would be necessary to develop a two- or three-dimensional model to determine exactly what would be predicted after loss of stability. The effect of the column walls would probably determine the ultimate nature of any maldistribution. Also, nonuniformity in the flow will produce macroscopic velocity and holdup gradients in the lateral direction. We expect that these will cause the viscous and pseudoturbulence stress terms in Eq. 3 to become important. It will be necessary to develop a better understanding of these terms before attempting to model higher-dimensional flow.

Another important observation can be made from the linear stability analysis. Rewriting Eq. 18 as

$$y^* = \hat{y} \exp [\gamma t + j\omega(z - ct)], \tag{28}$$

where $\gamma = Re(s)$ and $\omega c = -Im(s)$, we can identify $c = c(\omega)$ with the velocity of propagation of disturbances through the column. Our analysis revealed that, irrespective of whether the uniform state is stable or not, the waves propagate downwards in cocurrent downflow and in the lower branch of countercurrent flow. On the upper branch in the countercurrent flow, the waves propagate upwards. When instability occurs in cocurrent downflow, liquid-rich regions form and propagate downwards as linear stability analysis suggests (Grosser et al., 1988). This lends support to our supposition that, when an operating condition in the lower branch of the countercurrent flow loses stability, liquid-rich regions (if formed) will move downwards rapidly, as the velocities predicted by the linear stability analysis are much larger than the average liquid velocity in the column. This, in turn, implies that *the loss of stability of the lower branch does not imply the loss of operability (i.e., flooding)*. On the other hand, in the upper branch, the liquid slugs will propagate upwards and hence will result in liquid accumulation at the top of the column (i.e., flooding). Thus, loss of stability of the upper branch would result in loss of operability (without external controllers). The latter point is not profound, as the upper branch is made unattainable for other reasons which will be discussed when we consider a semiinfinite model.

Flooding

The definition of flooding given by Hutton and Leung (1974a) corresponds to the turning point of a constant liquid flux uniform state locus. Note that the derivative of gas flux with respect to liquid holdup is also zero at this point. If several liquid rates are examined, a family of curves can be generated, each with a characteristic limiting gas flux, G_{max}. If these limiting conditions can be identified with the flooding point, then it should be possible to compare the flooding conditions predicted from the uniform-state equation to a flooding correlation, such as that of Sherwood et al. (1938). Figure 7 shows such a comparison for the two models. Note that both models predict flooding at more severe conditions than the correlation. This is not surprising for the model using the Saez and Carbonell correlations, since they were developed from cocurrent downflow data. Hutton and Leung's correlations developed for countercurrent flow, however, also overpredict the flooding point. Similar deviations were reported in their original paper (Hutton and Leung, 1974a).

These large deviations suggest that the flooding observed by Sherwood et al. and other workers may not necessarily be identified with the limiting mass fluxes of the uniform-state curve in

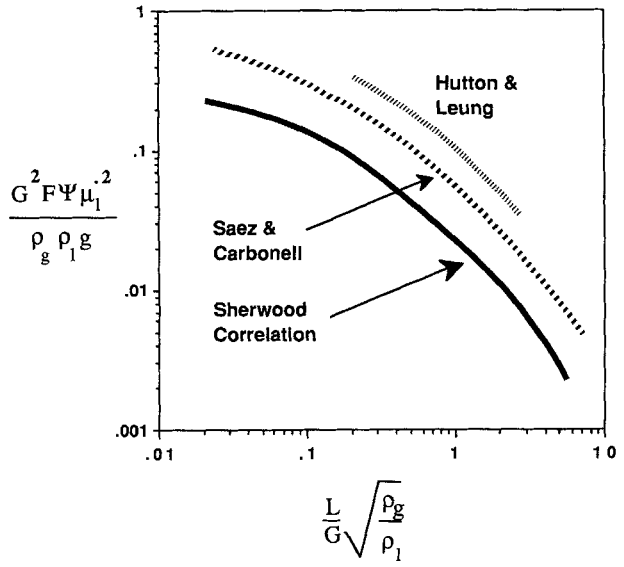

Figure 7. Comparison of the limiting condition, G_{max}, with the dimensionless flooding correlation of Sherwood et al. (1939).

The predictions for two drag force correlations are shown for 12.5-mm spherical packing.

the macroscopic model. Indeed, there are many opinions as to the precise point at which flooding occurs. Sometimes a sudden rise in pressure drop is used, while others use a visual criteria. Unexplained transient phenomena are also observed near the flooding point (Eckert, 1970; Elgin and Weiss, 1939).

Some other mechanism must be responsible for flooding at conditions less severe than the limiting uniform-state fluxes. The influence of the boundaries can be important especially in determining the flooding point, a factor which the uniform-state model ignores. Much attention is given in industry to the design of the support plate, as the flooding conditions can vary widely when different support plates are used.

Semiinfinite Model

The uniform state model for the interior of the bed should be relevant only when the top and bottom boundaries do not influence the flow far from the ends. In the case of support-plate-induced flooding, the bottom boundary of the bed apparently has a strong effect on the flow in the interior and renders a uniform-state model invalid. One method of studying this effect is to consider a semiinfinite model with bottom boundary conditions included. Instead of the uniform state, the steady-state holdup and pressure profiles must be calculated. The uniform state in an infinite bed can then be interpreted as an asymptotic limit to the steady-state profile far from the boundary. For countercurrent flow, our analysis predicted the possibility of two uniform asymptotic limits. Which one of these two uniform states is attained will depend on the holdup at the bottom of the column, which in turn will be dictated by the bottom distributor.

Steady-state operation can be described as the condition, when all time derivatives in the model equations vanish. Equations 1, 13 and 14 can easily be used to obtain the following relations for the steady-state liquid holdup and pressure gradient in a one-dimensional bed:

$$W_4 \frac{d\epsilon_l}{dz} = \frac{F_{lz}}{\epsilon_l} - \frac{F_{gz}}{\epsilon_g} + (\rho_l - \rho_g)g \tag{29}$$

$$\frac{dp_g}{dz} = -\frac{F_{gz}}{\epsilon_g} - \rho_g g - \frac{G^2}{\rho_g \epsilon_g^3}\frac{d\epsilon_l}{dz} \tag{30}$$

where W_4 is defined by Eq. 23. The z axis is chosen here to be pointing vertically upwards. Given appropriate boundary conditions, the above equations can be used to find the steady-state holdup and pressure profiles along a column. Strictly speaking, for countercurrent flow, one boundary condition will have to be specified at each end of the column. The assumption of incompressible gas phase, however, permits calculation of the steady-state holdup profile independent of the pressure gradient by integration of Eq. 29. Therefore, it is only necessary to specify the liquid holdup at the bottom of the bed to calculate the steady-state holdup in the interior of the bed for given external flow conditions.

The effect of the support plate can be interpreted physically as a tendency to hold a different volume fraction of liquid at the bottom when compared to the uniform state prevailing in the interior of the column. Visual observation of an operating column indicates that the liquid holdup is often slightly higher in the region just above the support plate. Also, the change in capillary pressure going from the interior to the exterior of the bed would tend to increase the liquid fraction at the support. The actual holdup at the support will probably vary with liquid and gas fluxes, and will depend on the geometry of the support plate. To study the effect of the support plate on the interior, let us consider a boundary condition describing the support-plate hydrodynamics as follows:

$$\epsilon_l(z = 0) = h_l^*(L, G, \text{etc.}) \tag{31}$$

Here $z = 0$ denotes the boundary at the bottom. The details of the function h_l will depend on the distributor geometry.

Since we are interested in the steady state, an understanding of the possible range of behavior in the column can be extracted by simply specifying a constant liquid holdup at the bottom as the boundary condition. The profiles resulting as this boundary value is changed will represent the range of possible profiles which could be observed. The values given by a particular hydrodynamic relation, such as Eq. 31, will be a subset of this range.

Equation 29 can be integrated numerically subject to condition 31 for various values of h_l^* to obtain the steady-state liquid holdup profiles. Figure 8 shows the results of such a calculation. For boundary holdup which is less than the lower uniform holdup, the profile rapidly approaches the lower uniform state. For bottom boundary holdup between the lower and upper uniform states, the profiles still approach the lower uniform state. As the boundary holdup gets near the upper uniform state, the elevated holdup persists for longer distances, but eventually falls to the lower uniform state. When boundary holdup is greater than the upper uniform state, however, the calculated steady-state liquid saturation rises rapidly to unity, at which point the numerical solution cannot be continued. This implies that no steady operation is possible for such high boundary holdup values. The upper uniform state can be obtained only if the holdup at the support

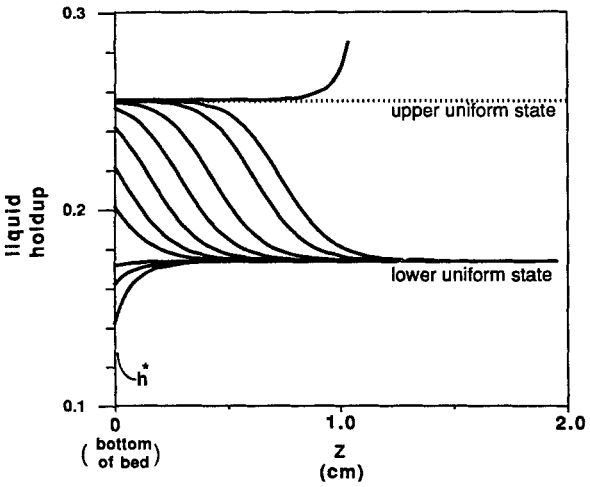

Figure 8. Typical steady-state liquid holdup profiles for several values of h^*.

The bottom of the bed corresponds to $z = 0$. $L = 5$ kg/m^2 · s, $G = 0.03$ kg/m^2 · s, $d_e = 3$ mm.

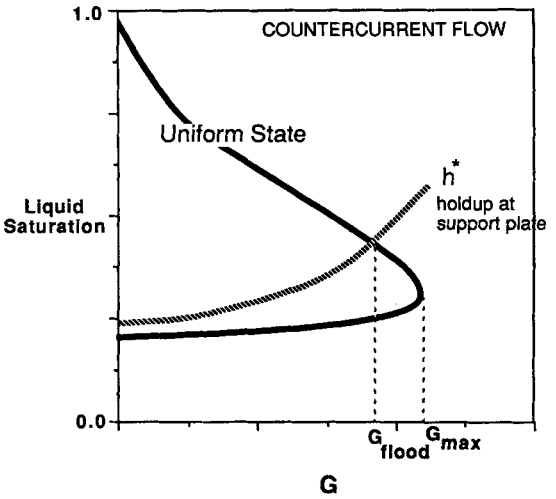

Figure 9. Proposed mechanism for support-plate-induced flooding.

The dashed curve represents holdup at the support plate. Flooding is induced at G_{flood}, which can be much less than the limiting condition G_{max}.

plate is exactly equal to the upper-state holdup, which is practically unlikely. It is for this reason that we discard the upper branch as physically unattainable (in the absence of external controllers).

Dr. Krambeck pointed out to us another heuristic argument for discarding the upper branch. If this branch were stable, then a small decrease in the liquid flux (Figure 3) in this branch, while holding G constant should lead to an increase in the liquid holdup—a requirement which is counterintuitive.

In every case, the liquid saturation either becomes uniform or diverges towards unity over the length of a few particle diameters. For conditions where bounded steady-state profiles exist, the interior of the bed is uniform and flow is not affected by the presence of a bottom boundary. For the case where the bottom holdup exceeds the upper uniform-state holdup, however, no steady-state profile exists, with the liquid holdup rapidly reaching the void fraction of the bed. As the holdup increases toward the liquid-full condition, the gas pressure will increase behind the obstructed region, carrying the extra liquid away. This would take the form of upward propagating regions of high liquid holdup. Indeed, linear stability analysis of the upper uniform state revealed that all waves will propagate upwards, as mentioned earlier. If this time-dependent condition is unstable, the bed will flood.

The steady-state profile results explain how the support plate can induce flooding prematurely in countercurrent packed beds. As the flow rate of one phase is increased, the holdup at the support will eventually exceed the upper uniform holdup, and the column will flood. If there is appreciable extra holdup at the support, this flooding can occur well before the flow rates have reached the limiting values corresponding to the uniform-state turning point. Figure 9 shows how this might happen at constant liquid flux. The solid curve represents the locus of uniform states, while the broken curve is a postulated holdup at the bottom support plate, h^*. In this illustration, at low gas flux the holdup at the support plate is only slightly higher than the lower uniform-state holdup. As gas flux increases, h^* also increases gradually. As long as h^* is less than the liquid holdup corresponding to the upper uniform state, the interior of the bed will be uniform. At some gas rate, G_{flood}, h^* may cross the upper uniform state branch. The interior of the bed is now suddenly affected by the bottom boundary, the entire bed changes to a higher holdup condition, and flooding occurs. The pressure drop across the bed would also exhibit a discontinuity at this point. Such sudden change in holdup and pressure drop with a small change in flux corresponds to the description of distributor-induced flooding given by Eckert (1970).

If the h^* vs. G locus (shown in Figure 9 by the broken line) is such that it always lies below the uniform state locus for $0 < G < G_{max}$, then no distributor-induced flooding will arise and true, column-limited flooding will be manifested. Also, the intersection of the h^* locus with the lower branch of the uniform-state locus does not signal any sudden transition. Thus, it is the upper branch of the uniform-state locus which plays a critical role in the occurrence of distributor-induced flooding. One sees that, although the upper branch itself is not spontaneously attainable in practice, this branch plays a significant, physically-important role in countercurrent flow through packed columns.

Upper-Uniform State

In the preceding discussion, we have used the shape of the uniform-state locus to reach several conclusions about the nature of the flooding point and the mechanism for support-plate-induced flooding. Most of these conclusions depend on the existence of the upper half of the uniform-state curve. Do these "upper" states exist in real packed columns? We mentioned in our discussion of stability and packing geometry that part of the upper branch of the curve can be stable in an infinite bed. In discussing the semiinfinite model, however, we showed that the upper branch was unattainable in an actual bed because of the presence of a boundary at the bottom. The last result implies that it will be impossible to observe the upper states as uniform-steady flow in a finite column.

Hutton and Leung (1974c) presented some evidence for the existence of a second hydrodynamic state. They examined the pressure drop and liquid holdup in a column that was induced to flood and then held in an almost flooded state by controlling the

gas rate. Flooding was induced with a restrictive support plate, allowing change of external flow rates by change of support-plate characteristics. The incipient flooding condition was associated with the upper hydrodynamic state predicted by their model. This conclusion was supported by experimental liquid holdup data which seemed to fall on the upper half of the curve, with lower gas rates leading to higher liquid holdup and pressure drop as predicted. They also concluded that the upper state is unstable, due to the tendency for any disturbance in liquid holdup to cause further deviation from the original point on the curve.

Hutton and Leung are not the first to report the incipient flooding mode of operation. Elgin and Weiss (1939) also observed a quasisteady, high holdup state at fluxes just below the limit of capacity of their column. They did not attempt to further characterize this state and did not consider the effect of their support plate, which appeared to be restrictive, since the flooding was always observed to begin at the bottom of the bed. They reported that the bed could be held indefinitely in the incipient flooding state by careful control of the gas flux.

Some experiments were performed in our laboratory in a two-dimensional bed packed with spheres. The apparatus used was essentially the same as described in Christensen et al. (1986). The experiments consisted mostly of pressure drop measurements and visual observations of flow phenomena. Appendix A provides details of the equipment and procedures employed. We have also been able to obtain the incipient flooding mode in our two-dimensional column. However, the flow we have observed is not uniform and steady, but is a transient state which exists near the flooding conditions where the column operates at significantly higher pressure drop and liquid holdup. The time-dependent nature of this state is characterized by pulses or wavelike regions of liquid which propagate up the bed. These waves travel upwards at speeds of about 0.5 to 1.0 m/s. They are similar in appearance and in speed to the downward traveling pulses observed in cocurrent trickle beds with the same type of packing.

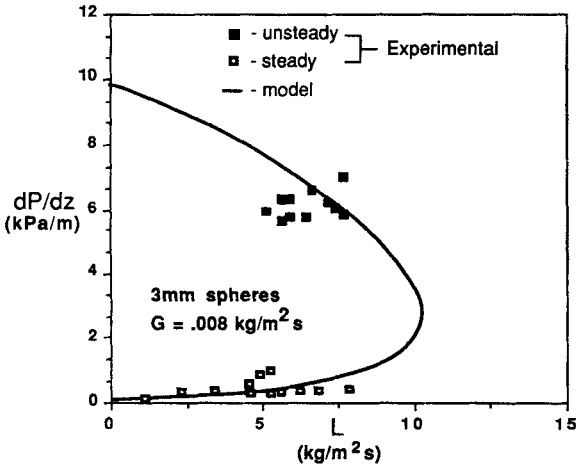

Figure 10. Comparison of the predicted uniform-state pressure gradient with measured pressure drop in a two-dimensional column for an air-water system.

The model curve uses the Saez and Carbonell drag force correlations.

Upper state data represent average pressure gradient during transient, time-dependent flow.

If the column is allowed to operate in this mode without careful control for a sufficiently long time, which ranges from minutes to hours, the column will eventually either subside to a low-pressure-drop uniform state or flood completely.

Similar wavelike behavior is reported by Elgin and Weiss (1939) for high gas rates, but not for high liquid rates. The pulses may have been unnoticeable in their bed, however, since their 6–12-mm packing was larger and had more voidage than our 3-mm spheres. It is known for cocurrent pulsing flow that the pulses have smaller amplitude as the packing size and bed porosity is increased.

The time-dependent, nonuniform flow observed in the incipient flooding mode cannot be identified with the upper uniform state. However, the average pressure gradient and holdup of this transient flow are very close to the corresponding properties of the upper uniform state from the model. This is demonstrated in Figure 10, which compares the pressure gradients for the upper branch predicted by the uniform state model with data from the two dimensional bed. The more extensive data given by Hutton and Leung (1974c) also provide evidence that the time-dependent regime is similar to the upper uniform state. The uniform-state conditions seem to act as an attractor for the time-dependent flow. In particular, the flow in regions between pulses seems to have the characteristics of the upper uniform state. The upward direction of propagation of the pulses is also predicted by the model.

We note in passing that in experiments with 3-mm spheres in a two-dimensional bed, we have found evidence that the average holdup and pressure drop are history-dependent and that countercurrent uniform flow exhibits the same type of hysteresis that has been observed in cocurrent trickling flow (Christensen et al., 1986). Typical data from an experiment of this type can be found in Appendix B. This behavior becomes very weak for larger packing sizes, explaining why such behavior has not been reported previously for countercurrent flow.

Summary

The hydrodynamics of two-phase countercurrent flow in packed columns can be analyzed using a simple macroscopic model. Properties such as liquid holdup and pressure gradient below the flooding point can be approximated by a uniform state where all temporal and spatial derivatives in the macroscopic equations vanish. The model predicts the existence of two uniform solutions, a low holdup state which is commonly observed below the flooding point and an upper, high holdup state. The lower solution corresponds qualitatively to the behavior observed experimentally. The upper state can be mathematically-stable for some conditions, but the presence of a boundary makes it inaccessible to steady flow. Although the boundary has a large effect on the flow when flooding is induced, the effect is negligible for conditions where the lower uniform state is attained.

The maximum (i.e., column-limited) flooding conditions can be identified as those beyond which no uniform state solution exists. This is equivalent to defining flooding as the condition where the bed will not allow any further increase in liquid or gas flux. Others factors can induce flooding at lower flow rates than predicted by the loss of existence of uniform-state solutions. In particular, the support plate can induce flooding by causing the holdup at the bottom of the column to exceed the holdup of the unstable upper solution. For restrictive support plates, this can

occur at fluxes substantially less than the maximum rates the bed will allow.

The stability of the uniform state can be affected by packing geometry and size. For large, high-voidage packing, no stable uniform solutions to the model equations are possible. This loss of stability at high bed voidage may represent the maldistribution of liquid which makes redistribution necessary in large industrial towers.

The macroscopic model obtained from volume averaging is quite general. The complexity of two-phase flow in packed columns, however, makes it all but impossible to deduce constitutive relations required in this model from purely first principles. Resorting to empiricism in formulating constitutive models for drag forces and capillary pressure is inevitable. An objection to the model immediately follows, and one wonders how the model can be superior to strictly empirical correlations already available in the literature for various hydrodynamic quantities such as liquid holdup and pressure drop in cocurrent and countercurrent flow, trickling-to-pulsing transition in cocurrent flow, etc. In strictly empirical treatment, different correlations are needed for different properties. The model would be credible and worthwhile if it can explain all the hydrodynamic phenomena and quantities with a small set of empirical quantities. Such a model may be extrapolated with greater confidence than purely empirical correlations.

Using empirical drag force correlations deduced from cocurrent trickling flow data (Saez and Carbonell, 1985) and Leverett's correlation for capillary pressure, Grosser et al. (1988) pointed out that one can explain trickling-to-pulsing transition from formal considerations. This is important, as one now has for the first time a model, albeit semiempirical, that can be used to simulate pulsing flow in cocurrent downflow, lateral segregation, etc.

The goal of the present study was to apply this model to countercurrent flow to examine whether it could bring forth three well-known phenomena in countercurrent flow: 1. flooding; 2. the strong influence of the bottom support plate on flooding; and 3. the occurrence of spontaneous segregation necessitating frequent liquid redistribution in some columns. We have demonstrated in this paper that this model can indeed explain these phenomena quite elegantly and have also brought forth the reasons for the occurrence of these phenomena. Herein lies the contribution of the present study.

The success of the simple semiempirical model in predicting in a qualitatively correct manner the features of both cocurrent and countercurrent flow through packed beds lends credibility to the model itself. At the present time, it appears reasonable to hope that an improvement in our understanding of the pulsing flow in cocurrent downflow and lateral maldistribution in both cocurrent and countercurrent flows may come about from an analysis of the time-dependent model equations in multidimensions.

Acknowledgments

Financial support for David C. Dankworth from the Fannie and John Hertz Foundation through a graduate fellowship is gratefully acknowledged. We would also like to thank Roy Jackson and Fred Krambeck for their helpful comments and questions.

Notation

A, B = Ergun constants
a_v = volume to surface area ratio for packing, 6/dia. for spheres
d_e = particle diameter
Eo^* = Eotvos number, Eq. 7
$\underline{F}_i$, $i = l, g$ = total drag force per unit bed volume experienced by phase i
F_{iz}, $i = l, g$ = drag force per unit bed volume experienced by phase i in the axial direction
F = shape factor for the Sherwood correlation $6/(d_e\epsilon^3)$
g = acceleration due to gravity
G = gas-phase mass flux
h^* = liquid holdup at the bottom of the bed

Liquid holdup at the bottom of the bed

i = the square root of -1
$J(\epsilon_l)$ = Leverett J-function
(ϵ_l) = $dJ/d\epsilon_l$
k = permeability of the packed column
L = liquid-phase mass flux
p_i, $i = l, g$ = pressure in phase i
p_c = capillary pressure
$\boldsymbol{R}_i$, $i = l, g$ = pseudoturbulence stress tensor for phase i
$s_l = \epsilon_l/\epsilon$, liquid saturation
S' = packing factor in Eq. 9
t = time
u_i, $i = l, g$ = local mean velocity of phase i
W_1–W_5 = see Eqs. 20–24
y = symbol for a state variable in Eq. 18
z = axial distance

Greek letters

α_i, β_i, $i = l, g$ = see Eq. 25
ϵ = porosity of the bed
ϵ_i, $i = l, g$ = volume fraction of phase i in the bed
ϵ_l' = residual, or static liquid holdup
ρ_i, $i = l, g$ = density of phase i
μ_i, $i = l, g$ = viscosity of phase i
σ = interfacial tension
τ_i, $i = l, g$ = viscous stress tensor for phase i
Ψ = density ratio in the Sherwood correlation $(\rho_{l_i}/\rho_{water})$
ω = wave number of imposed disturbance

Superscript

o = uniform steady state

Literature Cited

Buchanan, J. E., "Holdup in Irrigated Ring-Packed Towers below the Loading Point," *I&EC Fund.*, **6**, 400 (1967).
Christensen, G., S. J. McGovern, and S. Sundaresan, "Cocurrent Downflow of Air and Water in a Two-Dimensional Packed Column," *AIChE J.*, **32**, 1677 (1986).
Davidson, J. F., "The Holdup and Liquid Film Coefficients of Packed Towers: II. Statistical Models of the Random Packing," *Trans. Instn. Chem. Engrs.*, **37**, 131 (1959).
Eckert, J. S., "Design Techniques for Sizing Packed Towers," *Chem. Eng. Prog.*, **57**(9), 54 (1961).
Eckert, J. S., "Selecting the Proper Distillation Column Packing," *Chem. Eng. Prog.*, **66**(3), 39 (1970).
Elgin, J. C., and F. B. Weiss, "Liquid Holdup and Flooding in Packed Towers," *Ind. Eng. Chem.*, **31**, 435 (1939).
Grosser, K. A., R. G. Carbonell, and S. Sundaresan, "The Onset of Pulsing in Two-Phase Cocurrent Downflow through a Packed Bed," *AIChE J.*, **34**, 1850 (1988).
Hutton, B. E. T., L. S. Leung, P. C. Brooks, and D. J. Nicklin, "On Flooding in Packed Columns," *Chem. Eng. Sci.*, **29**, 493 (1974a).
Hutton, B. E. T., and L. S. Leung, "Cocurrent Gas-Liquid Flow in Packed Columns," *Chem. Eng. Sci.*, **29**, 1681 (1974b).
Hutton, B. E. T., and L. S. Leung, "A New Mode of Countercurrent Gas-Liquid Flow in Packed Columns," Australasian Conf. on Hyd. and F.M., 477 (1974c).
Jesser, B. W., and J. C. Elgin, "Studies of Liquid Holdup in Packed Towers," *Trans. AIChE*, **39**, 277 (1943).

Leverett, M. C., "Capillary Behavior in Porous Solids," *Trans. AIME*, **142**, 159 (1941).
Lobo, W. E., L. Friend, F. Hashmall, and F. A. Zenz, "Limiting Capacity of Dumped Tower Packings," *Trans. AIChE*, **41**, 693 (1945).
Reed, A. W., H. Meister, and J. Sasmor, "Measurements of Capillary Pressure in Urania Debris Beds," *Nucl. Tech.*, **78**, 54 (1987).
Saez, A. E., and R. G. Carbonell, "Hydrodynamic Parameters for Gas-Liquid Cocurrent Flow in Packed Beds," *AIChE J.*, **31**, 52 (Jan., 1985).
Sherwood, T. K., and H. Shipley, "Flooding Velocities in Packed Columns," *Ind. Eng. Chem.*, **30**, 765 (1938).

Appendix A: Experimental Apparatus and Procedure

Some experiments were undertaken to obtain data for smaller packing sizes. The two-dimensional column described by Christensen et al. (1986) was modified to operate in the countercurrent regime. The Plexiglass-walled, rectangular column had internal dimensions of 0.051 × 0.457 × 1.83 m. Alumina beads of 3-mm and 6-mm nominal diameter were used as packing. The bed was filled with dry beads up to 0.3 m of the top distributor. Tap water was employed as the liquid phase and was distributed in two stages over the top of the bed. The primary distributor was a horizontal pipe with holes in its sides, positioned across the column. The secondary distributor was a plate with 75 4.8-mm copper tubes, inserted just below the primary distributor. Five 11-mm tubes were also installed in the secondary distributor to allow the air to pass out of the column through the vent on the top. The air was cooled and filtered before entering the side of the column just below the support plate. No humidification was performed. Both phases were metered to the column through a series of valves and rotameters. A 0.3 m disengaging space was provided at the bottom of the column to allow free flow of gas into the entire cross section. A water level was maintained in the disengaging space by means of a gate valve which controlled the water draining out of the column to be recirculated.

The pressure drop was measured through differential pressure transducers mounted across a 0.3 m section of the column located midway between the top and bottom of the packed bed. The transducer output was monitored with a digital voltmeter for uniform flow and with a chart recorder during transient operation. The transducers were calibrated before each experiment by filling the entire bed with water and bleeding water through the transducer chambers on both sides of the diaphragm. This also served to thoroughly wet the packing before beginning flow experiments.

Careful attention was given to the design of the support plate at the bottom of the bed. The support plate was found to have a very large influence on the fluxes necessary to flood the column. Three support plates were used for the 3-mm particles. A plain wire mesh grid with 6-mm openings covered by a 3-cm layer of 6.4-mm ceramic raschig rings was found to produce flooding at gas rates about one half of those needed to flood the bed when a mesh with 2-mm openings, which was bent into 1.5-cm corrugations, was employed.

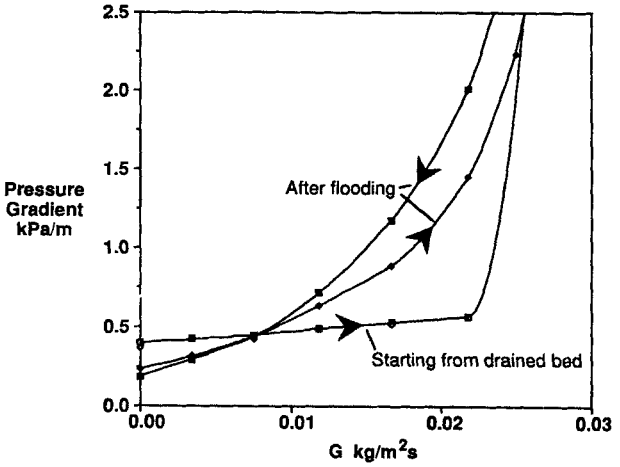

Figure A1. Experimental evidence for pressure drop hysteresis in countercurrent flow through a bed of 3-mm alumina beads.
Data points are shown for a typical experimental sequence. The curves are drawn between consecutive measurements, and arrows show the direction of change. $L \approx 7.7$ kg/m² · s.

Appendix B: Experimental Evidence for Pressure Drop Hysteresis

Figure A1 shows experimental data for pressure gradient vs. gas mass flux collected in the two-dimensional column packed with 3-mm alumina spheres and using the corrugated support plate. The curves trace the direction of changing gas flux during the experiment. At the start of the experiment, the bed was allowed to drain for ten minutes. After liquid flow was established at 7.7 kg/m² · s, the gas rate was slowly increased. Initially, the pressure gradient followed the lower curve in Figure A1, with very little change in pressure gradient until the bed suddenly flooded. After flooding, the gas rate was decreased in intervals back to zero. The pressure gradient on the return from flooding is shown by the upper curve with the downward pointing arrow in Figure A1. Without stopping the liquid flow, the gas rate was then increased in intervals. The pressure gradient was observed to follow the middle curve in Figure A1, with a smooth transition into flooding. Subsequent cycles of changing the gas rate between zero and flooding conditions gave pressure gradients which fell within the two upper curves. If the liquid flow was shut off and the bed allowed to drain for five minutes, the pressure gradient on resuming the experiment would again follow the lower curve and would resume the upper hysteresis cycle only after flooding had occurred. The lower curve, observed only when the experiment was started from a well drained bed, probably shows the presence of rivulet flow. After flooding, the liquid distribution in the bed would be more uniform, and thus a larger pressure gradient is observed.

Manuscript received Mar. 6, 1989, and revision received May 19, 1989.